Polyoxometalates/polymer composites for the photodegradation of bisphenol-A

Chaima Brahmi, Mahmoud Benltifa, Mariem L Ghali, Frédéric Dumur, Corine Simonnet- Jégat, Valérie Monnier, Fabrice Lalevée Morlet-Savary, Latifa Bousselmi, Jacques Lalevée

L PAPER

Polyoxometalates/polymer composites for the photodegradation of bisphenol-A

Chaima Brahmi, [a,b,c,d] Mahmoud Benltifa*,[c] Mariem Ghali, [a,b,c,d], Frédéric Dumur,[e] Corine Simonnet-Jégat,[f] Valérie Monnier,[g] Fabrice Morlet-Savary,[a,b] Latifa Bousselmi,[c] Jacques Lalevée*[a ,b]

[a] C. Brahmi, M. Ghali, Dr. F. Morlet-savary, Prof. J. Lalevée
Mulhouse Materials Science Institute (IS2M, CNRS)
Haute-Alsace university (UMR 7361)
F-68100 Mulhouse, France
E-mail: Jacques.lalevee@uha.fr
[b] C. Brahmi, M. Ghali, Dr. F. Morlet-savary, Prof. J. Lalevée
Strasbourg university
F-67000 Strasbourg, France
[c] C. Brahmi, Dr. M. Benltifa, M. Ghali, Prof. L. Bousselmi
Laboratory of Wastewaters and Environment
Center for Water Research and Technologies (CERTE)
BP 273, Soliman 8020, Tunisia
E-mail: mahmoud.benltifa@certe.rnrt.tn
[d] C. Brahmi, M. Ghali
National Institute of Applied Sciences and Technology
University of Carthage
Tunis 1080, Tunisia
[e] Dr. F. Dumur
Aix Marseille Univ, CNRS, ICR, UMR7273,
F-13397, Marseille, France
[f] Dr. C. Simonnet-Jégat
Lavoisier Institute of Versailles, UMR CNRS 8180,
University of Paris Saclay, University of Versailles St-Quentin en Yvelines,
F-78035, Versailles, France
[g] Aix Marseille Univ, CNRS, Fédération des Sciences Chimiques de Marseille, F-13397, Marseille, France

Supporting information for this article is given via a link at the end of the document.

Abstract: To satisfy the demands of people for clean and safe water, new technologies for wastewater treatment have been developed. Hence, photocatalysis has emerged as a green chemical approach for such treatment. In this context, we have developed a new regenerable POM/polymer composite characterized by photocatalytic properties which are synthesized by photopolymerization process under mild conditions. Furthermore, the photocatalytic ability of these new hybrid materials has been applied for water treatment in order to remove different emergent pollutants such as dyes and organic compounds. In fact, the POM excited by the irradiation could oxidize directly the pollutants adsorbed on its surface or generate highly reactive chemicals such as °OH radicals which promote the degradation. In order to increase the conversion rates of these pollutants, different sources of irradiation have been used. The most efficient were the UV lamp and the solar irradiation. Pollutants degradation mechanisms as well as identification of the photoproducts will be discussed using mass spectroscopy technique.

Introduction

Bisphenol-A (BA) is an endocrine disrupting chemical (EDC) and an emerging pollutant, manufactured worldwide in high quantities. This compound is mainly used in polymer science for the production of polycarbonate and epoxy resins[1]. As example, Bisphenol-A is used to synthesize food and water containers, coating materials for cans, baby bottles, water pipes, sports equipment, eyeglasses lenses, consumer electronics. It is also used for dental fillings, paints, medical equipment and different types of paper and cardboards including cigarette filters and cash register receipts[2]. The Bisphenol-A can be released from these plastics products under existing conditions, therefore high heat, alkaline and/or acidic conditions can promote his release into different environments including air, soil and more especially water.

The water is the most important resource for living species. However, potable water which is indispensable for every human being represents only 1% of surface water from lakes and rivers[3]. In fact, wastes of Bisphenol-A which are generated during his production or transport processes and after the massive use of plastic products is continuously introduced with different concentrations into the aquatic environment via municipal wastewater and manufacturing discharges[4]. Indeed, it was detected in surface water with concentrations equal to 7.3 ng/L in Léman French lake[5] and between 28.7-98.4 ng/L and 4–92 µg/L in Portuguese and Germany rivers, respectively[6,7]. This endocrine disruptor appears also at higher concentration ranging from 0.23 to 149.2 µg/L in Canadian industrial effluents[8].

Because of the high production and application of Bisphenol-A in various products, several toxic impacts of this chemical exposure were spread onto all the living being especially humans. In fact, a prenatal exposure to this chemical causes fetus and children neurodevelopment disorders such as autism[9]. Moreover the penetration of Bisphenol-A into the humans bodies by dietary ingestion, inhalation or skin contact threats humans health by causing several diseases including cancer[2,10],diabetes, obesity[11] and cardiovascular problems such as angina, hypertension and heart attack [12]. Additionally, many studies have proved that exposure to Bisphenol-A affects humans reproductive

systems[13],15,16]. Bisphenol-A has also attracted many researchers' interest since 2000. Based on first bibliometric analysis, the number of publications related to this pollutant have continuously increased with approximately 284 publications per year and reached a total of about 70,000 articles in 2019 (Figure 1, curve (A)), proving the enormous interest brought to this chemical and its negative effects clearly identified by the scientific community. Due to these harmful and toxic effects, Bisphenol-A have captivated the attention of several regulatory agencies, such as the European Food Safety Authority (EFSA) who decreased the tolerable daily intake (TDI) for BA from 50 to 4 µg/kg per bodyweight day[16].

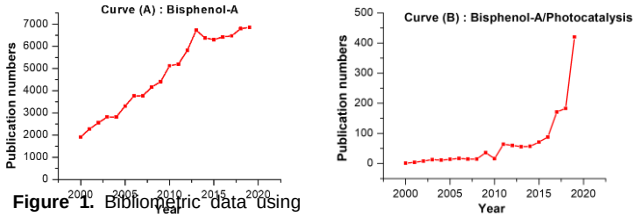

Figure 1. Bibliometric data using the keywords: Bisphenol-A (curve (A)) and Bisphenol-A/Photocatalysis (curve (B)). Source: BibCNRS

To mitigate the harmful effects of this pollutant on the environment and especially in water, several processes to remove this compound have been developed including adsorption[17,18], electrochemical process[19,20], chlorination[21,22], biodegradation[23–25] and advanced oxidation methods (AOP) which are based on powerful oxidants as the radical °OH[21]. However, in the case of BA chlorination and ozonation, several studies have reported the formation of toxic intermediates[27,28]. Moreover, all these methods are expensive to use for the removal of these pollutants.

Among AOP, photocatalysis has emerged as a promising technique for the treatment of bio-recalcitrant pollutants. In fact, high degradation and mineralization rates of Bisphenol-A can be achieved by using photocatalytic oxidation[29]. In this context, the same bibliometric analysis demonstrated high interest to this process for BA degradation (Figure 1(curve (B)). About 1186 articles have been published since 2000 on the Bisphenol-A photocatalytic degradation by various developed and improved photocatalysts including bismuth, silver, zinc and carbon based photocatalysts[6,24]. High increase was observed since 2015 and publications number doubled between 2018 and 2019, showing that photocatalysis is an innovative degradation process for this organic pollutant. The degradation performance of Bisphenol-A by photocatalysis is summarized in Table 1. As treatment conditions, irradiation intensity, treatment time and photocatalyst type vary widely from one publication to another, a ratio B* representing the "average degradation" was calculated by considering Bisphenol-A degradation percentages, initial concentration of BA, the treated volume and reaction time is used for comparison. The apparent Kinetic order can be also used for this purpose when available. Others parameters are also important such as the catalyst amount and the specific surface of the catalyst. It appears that the "average degradation" vary widely from $2*10^{-6}$ mg.min^{-1} to 1.30 mg.min^{-1}, with interesting values using only sunlight[31,32].

Table 1. Comparative study of the different suspended photocatalysts used for Bisphenol-A photodegradation.

Photocatalyst	Light source	Average degradation (mg.min^{-1}) (B*)	Catalyst amount (mg/L)	Specific surface (m^2/g)	Kapp (min^{-1})	Ref.
ZnO/carbon xerogel	Solar irradiation	1.30	500	24.4	0.0051	[31]
TiO_2-SiO_2	500 W halogen lamp	$1.08*10^{-1}$	500	49	0.121	[33]
TiO_2@ACD @RGO	250 W metal halide lamp	$3.47*10^{-2}$	1000	83.83	0.739	[34]
WO_3/TiO_2	150 W Hg lamp	$2.5*10^{-2}$	62.5		-	[35]
Ag/AgCl/Fh /H_2O_2	5 W LED light	$2.5*10^{-2}$	1000		0.0506	[36]
g-C_3N_4/MoS_2-PANI	Visible light	$1.57*10^{-2}$	-	184.21	0.0395	[37]
TiO_2/nano-diamond	20-W Omnilux lamp	$1*10^{-2}$	80		6.66*10-4	[38]
(CNQDs)/TiO_2	Xenon lamp	$6.25*10^{-3}$	1000	37.06	3*10-1	[39]
Pd@MIL-100(Fe) /H_2O_2	300 W Xe lamp	$5.30*10^{-3}$	125	2102	-	[40]
(0,3AF-C_3N_4)	Visible light λ > 420 nm	$3.89*10^{-3}$	200	46	$1.02*10^{-2}$	[41]
ZnO/MIL-100(Fe)/H_2O_2	500 W Xe lamp	$3.1635*10^{-3}$	200	654	-	[42]
Bi/Bi_2WO_6	500 W xenon lamp	$2.997*10^{-3}$	250	-	$3.67*10^{-4}$	[43]
S-TiO_2/UiO-66-NH_2	Visible light LED 50 mW	$2.026*10^{-3}$	200	154.26	$2.98*10^{-2}$	[44]

Cu-ZnO	Two halogen lamps	$2.06*10^{-3}$	50	49	$7.6*10^{-3}$	[45]
$ZnFe_2O_4$	Sunlight	$3.19*10^{-4}$	2000		$7.06*10^{-2}$	[46]
ZnO@ZnHCF	Sunlight	$3.23*10^{-5}$	926	113.491	4*10-3	[47]
WO_3/MIL-100(Fe)/H_2O_2	25 W LED light	$2*10^{-6}$	250		-	[48]

B* was calculated by this paper's authors.

In this context, Polyoxometalates (POM) have appeared as a new visible-light photocatalysts thanks to their low toxicity and cost, their acidity and redox properties as well as their efficient absorption of the light at a wider wavelength domain than that obtained with TiO_2 [49,50] .These appealing properties have made POMs, interesting photocatalysts for the degradation of pollutants including photocatalytic reduction of toxic metals[51], isolating toxic gases[52] as well as photocatalytic oxidation and mineralization of a variety of pollutants such as pesticides[53], dyes[52,54,55] and organic pollutants including chlorophenols[56], ibuprofen[57], formic acid[55] and sulfamethoxazole[55]. Remarkably, according to the same bibliometric analysis, only two papers[58,59] have been published on the Bisphenol-A photocatalytic degradation by suspended polyoxometalates. However, these clusters are very soluble in aqueous solutions, which limit their recyclability and their reuse as a photocatalyst and introduce an organic pollution to the treated environment. As a solution, several studies have reported the association of POMs with counter ion[60], TiO_2[61], silica gel[62] or active carbon[63].

Recently, immobilization of POMs into polymers has been achieved in our previous works[64,65]. Different POM/polymer composites were synthesized by photopolymerization upon visible light and the photocatalytic abilities of these materials have been proved as well as their regeneration. The photodegradation mechanism is based on the creation of electrons and holes by exciting the POM under near UV light irradiation. The POM excited by the irradiation could oxidize directly the pollutants adsorbed on its surface or generate highly reactive chemicals such as °OH radicals, promoting the degradation[64]. The objective of this paper is to apply these novel photocatalysts to the degradation of the BA and to optimize the operating parameters for high degradation rate. The removal of this pollutant from aqueous solution will be investigated under different sources of irradiation and by using different synthesized composites. Pollutant degradation mechanism as well as identification of the photoproducts was discussed using mass spectroscopy technique.

Results and Discussion

Study of Bisphenol-A photodegradation in water by UV-Vis spectrometry

First, BA photodegradation kinetics were monitored by UV-Visible spectrometry in the presence or not of the phosphomolybdic composite and under different irradiation sources including UV lamp, LED@375nm and sunlight (Figure 2).

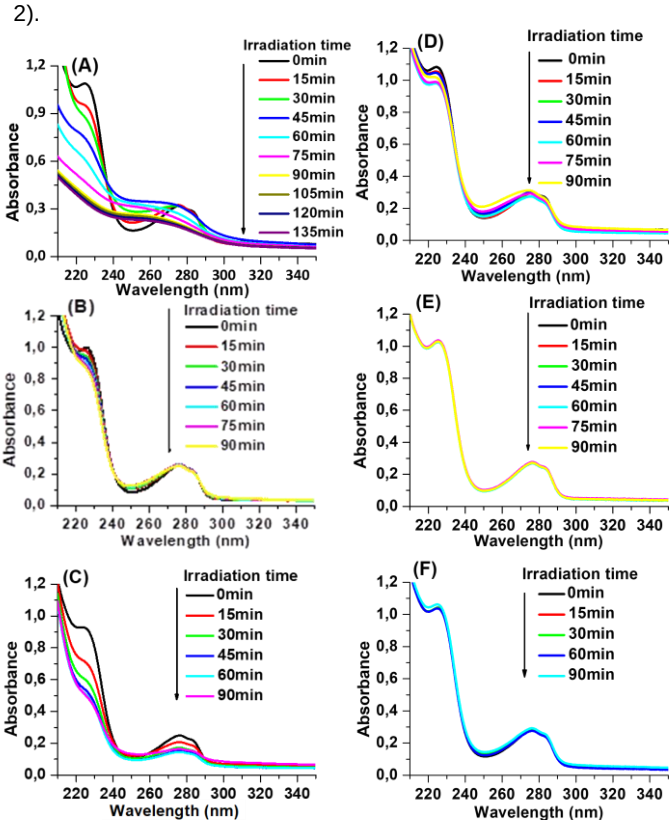

Figure 2. UV-visible absorption spectra of Bisphenol-A (15 ppm) in water at different irradiation times in the presence of $H_3PMo_{12}O_{40}$/polymer (BAPO/Iod) composite under: (A) UV lamp; (B) LED@375nm; (C) solar irradiation and without photocatalyst and under (D) UV lamp; (E) LED@375nm; (F) Solar irradiation. Initial pH=6.5.

The BA photolysis absorption spectra in water in the absence of the composite at different irradiation times using various sources of irradiation shown in Figure 2 (D, E and F), indicates almost no temporal changes of the absorption peak of this pollutant. This result indicates that the BA dissolved in pure water did not photolysis under any of the used irradiation source.

However, Figure 2 (A, B, C) show that the absorption peaks of BA, were gradually reduced with increasing the irradiation time using the same sources of irradiation in the presence of $H_3PMo_{12}O_{40}$/polymer composite due to the photocatalytic reaction. Indeed, the obtained conversion rates presented at Figure 3, show that after 90 min of irradiation, the different light sources efficiencies for BA removal from low to high were the LED@375nm (50.3%), the sunlight (88.2%) and the UV Lamp

(100%), respectively. According to Table 7, the band gap of the composite can be excited by the three irradiation sources based on their respective wavelength domains. The excitation of POM encapsulated into the composite produces hydroxyl and peroxide radicals which oxidize BA. The BA adsorbed on its surface can also react directly with the produced e^-/h^+ at the surface of the composite[64].

The reason for the high degradation rates achieved upon application of the photocatalytic system under solar (766 mW/cm^2) and UV lamp irradiations (250 mW/cm^2) are due to a larger excitation domain and a higher intensity compared to the LED source (70 mW/cm^2).

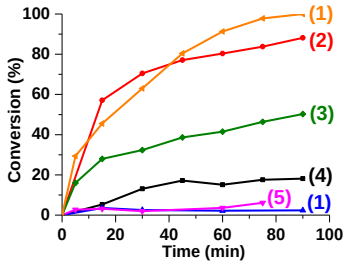

Figure 3. Conversion of Bisphenol-A in the presence of the composite under (1) UV Lamp, (2) sunlight, (3) LED@375nm, and without the composite under (4) UV Lamp, (5) sunlight and (6) LED@375nm. $[BA]_0$=15 ppm, pH=6.5.

In fact, an increasing the power of the UV lamp induces an improvement on BA degradation reaching 100% after 90 min of 250 mW/cm^2 irradiation (Figure 4 ((A) and (B)). The conversion rate increases linearly with the intensity. Such observations have also been reported in the literature by Son et al. who studied the degradation of BA[66] and by Pirgholi-Givi et al. who applied titanium dioxide nanostructures for the removal of Methylene Blue from water under different sources of irradiation[67]. Aguado et al. have also noticed that photocatalytic reaction kinetics is proportional to the irradiation source intensity and to the square root of light intensity if this one is beyond 250 W/m^2 [68].

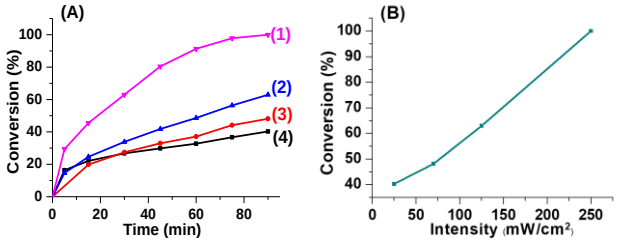

Figure 4. (A) Photodegradation of Bisphenol-A as a function of time, at various UV lamp Intensity in the presence of $H_3PMo_{12}O_{40}$/polymer composite in water: (1) 250 mW/cm^2; (2) 125 mW/cm^2; (3) 70 mW/cm^2 and (4) 20 mW/cm^2. (B) Effect of the intensity of irradiation on the conversion rate of Bisphenol-A in the presence $H_3PMo_{12}O_{40}$/polymer composite in water.

The efficiency of the $H_3PMo_{12}O_{40}$/polymer composite was compared to that of $W_{10}O_{32}(TH)_4$/polymer composite and to Titanium dioxide/polymer as TiO_2 is the most widely used photocatalyst nowadays under UV light. All composites were synthesized under the same operating conditions (Figure 5).

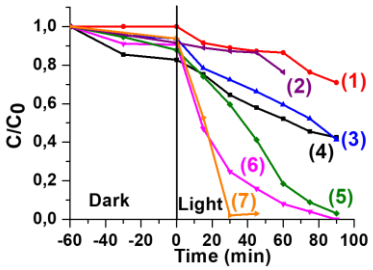

Figure 5. Bisphenol-A photolysis (1) without photocatalysts presence and in the presence of (2) Suspended TiO_2, (3) TiO_2/polymer composite, (4) Polymer, (5) $W_{10}O_{32}(TH)_4$/polymer composite, (6) $H_3PMo_{12}O_{40}$/polymer composite and (7) Suspended $W_{10}O_{32}(TH)_4$, under UV lamp irradiation. $[BA]_0$=15ppm, pH=6.5.

In the dark (Figure 5), phosphomobolybdic and decatungstate composites show limited ability to adsorb BA in the dark compared to the polymer without catalysts which adsorbs the highest quantity of BA (18%). This better adsorption is ascribed to the larger BET surface area of 9.3 m^2/g comparing to the decatungstate and phosphomolybdic composites which have a BET surface area of 5.4 m^2/g and 1.32 m^2/g respectively (Table 7). Moreover, approximatively 10% and 6% of BA are adsorbed respectively by 0.53 g/L of suspended TiO_2 and $W_{10}O_{32}(TH)_4$, comparing to 13% and 7% adsorbed respectively by $W_{10}O_{32}(TH)_4$/polymer and TiO_2/polymer composites.

Under irradiation, Figure 5 shows a comparative study between the different synthesized materials as well as the suspended catalysts used for the BA removal. The two POM/polymer composites exhibit a high BA photocatalysis under UV lamp irradiation. In fact, approximately 100% and 95% of this compound is removed by $H_3PMo_{12}O_{40}$/polymer and $W_{10}O_{32}(TH)_4$/polymer composites, respectively after 1 hour of irradiation. The most efficient photocatalyst was the phosphomolybdic composite, which is more easily reduced than the decatungstate composite, thanks to the higher redox potential of the molybdate POM (approximatively a difference of 0.4V)[69,70]. Furthermore, a molybdate kegging type polyoxometalate can accept between 1 e^- and 12 e^-, however, the decatungstate can accept only 1 or 2e^-[70].The decatungstate composite is also more efficient than titanium dioxide/polymer composite despite a similar band gap. This high removal percentages are achieved thanks to the polyoxometalates redox properties.

The in situ embedded photocatalyst in the composite has a lower efficiency compared to the suspension. This behavior is confirmed in the case of decatungstate POM, which removed 100% of BA in 30 min under UV lamp irradiation when it is used in suspension (Figure 5 (curve 7)) vs. 41% in composite (Figure 5

(curve5)). On the contrary, for the titanium dioxide, its presence in composite increases its efficiency to 41% after 60 min of treatment. (Figure 5 (curves 2 and 3)) vs. 24% in suspension. This improvement of the conversion rate suggests a better TiO_2 photocatalytic behavior in the polymer.

The kinetics of BA photolysis and photodegradation by the different developed materials was quantitively investigated by fitting the zero order, pseudo first-order and pseudo second-order equations to the experimental data. These models are given by the following equations[71]:

$$C_0\text{-}C = k_{app,0}\, t \quad (1)$$

$$-Ln(C/C_0) = k_{app,1}\, t \quad (2)$$

$$(C_0\text{-}C)/(C*C_0) = k_{app,2}\, t \quad (3)$$

C and C_0 designate respectively the BA initial concentration and at time t, $k_{app,0}$ is the zero-order rate constant (mg $L^{-1}min^{-1}$), $k_{app,1}$ is the first-order rate constant (min^{-1}), $k_{app,2}$ is the second-order rate constant (L mg^{-1} min^{-1}) and t the time. Therefore, k_{app} gives an indication of the activity of the catalyst. Results are shown in Table S1.

As shown in Table S1, regression coefficients (R^2) calculated based on the zero order and second-order reactions, are very low and ranged from 0.771 to 0.976 and from 0.563 to 0.9924, respectively, thus displaying that BA degradation by the different developed composites does not follow the zero-order and pseudo-second-order kinetics. However, the experimental data exhibits a good fitting with the pseudo-first-order kinetic since the calculates regression coefficients varied between 0.955 and 0.998 confirming that BA is degraded by the different synthesized photocatalysts according to this kinetic model.

In order to evaluate the newly developed POM/polymer composites efficiencies on the BA photodegradation under UV illumination, we have compared this pollutant average degradation, the active surface area and the photocatalyst amount fixed at the material surface of the synthesized composites with the different immobilized photocatalysts reported in the literature (Table 2). Therefore, a coefficient D* representing the ratio between average degradation and the active surface area of the immobilized photocatalysts, was calculated (Table 2: coefficient D*).

Table 2. Comparative study of the different immobilized photocatalysts used for Bisphenol-A photodegradation.

Photocatalyst	Light source	D* [a]	Catalyst amount (mg)	Specific surface area (m^2/g)	k_{app} (min^{-1})	References
$H_3PMo_{12}O_{40}$/polymer composite	UV light	$3.55*10^{-4}$	1.6	1.3	$4*10^{-2}$	This work
	Sunlight	$3.13*10^{-4}$	1.6	1.3	-	
$W_{10}O_{32}(TH)_4$/polymer composite	UV light	$3.37*10^{-4}$	1.6	5.4	$3.67*10^{-2}$	This work
TiO_2/polymer composite	UV light	$1.77*10^{-4}$	1.6	-	$8.2*10^{-3}$	This work
TiO_2–BHFM (bauxite-based hollow fiber membrane)	UV light (30W	$4.33*10^{-6}$	-	-	-	[72]
	Visible light	$2.89*10^{-6}$	-	-	-	
TiO_2	Solar simulator	$2.53*10^{-3}$	339	15-25	$15*10^{-3}$	[73]
ZnO immobilized on glass plates by a heat attachment method		$2.84*10^{-3}$	15.3	50	$11*10^{-3}$	
Au/ZnO hybrid inverse-opal	simulated solar light	$1.67*10^{-4}$	3500	21.2	-	[74]
Fe_2O_3/g-C_3N_4@N-TiO_2 nanotubes	Simulated sunlight	$1.86*10^{-3}$	-		$3.34*10^{-2}$	[75]
0.15 BiOI/ZnO NRs immobilized Indium tin oxide (ITO) glass	visible-light irradiation	$9.27*10^{-4}$	10	-	-	[76]
			10	-	-	

[a] Average degradation/Material active surface ($mg.min^{-1}.cm^{-2}$). D* was calculated by this paper's authors.

The most relevant photocatalysts were identified by the highest ratios between the average degradation and the catalyst amount. The most distinguished high-performing ones are the ZnO or TiO_2 catalysts powders immobilized on glass plates by a heat attachment method[73] and the BiOI/ZnO NRs immobilized on an Indium tin oxide (ITO) glass (1.5 × 3.0 cm^2) by a solvothermal process[76] used respectively under solar simulator accompanied by an ultrasonic radiation and visible-light irradiation (Table 2). Interestingly, we have noticed that the photocatalysts efficiencies didn't depend only on their amount or their active surface area but also on the chosen irradiation source.

Furthermore, results reported in Table 2 show also that ratio between BA average degradation and photocatalysts active surface area (coefficient D*) of the Fe_2O_3/g-C_3N_4@N-TiO_2 nanotubes[75], 0.15 BiOI/ZnO NRs[76], TiO_2 and SiO_2 immobilized on glass plates[73] are higher than those of the POM/polymer composites which could reflect a better photocatalytic ability.

However, the photocatalysts amount used for the development of those materials are much higher than the POM quantity used here for the POM/polymer composites synthesis. In fact, an average degradation of $6.66*10^{-4}$ mg.min^{-1} is achieved by using a 1.88 cm^2 pellet containing just 1.6 mg of $H_3PMo_{12}O_{40}$ or $W_{10}O_{32}(TH)_4$. However, BA is degraded at $6.39*10^{-3}$ mg.min^{-1} by 15.3 mg of ZnO fixed into 2.25 cm^2 glass plates which is one of the most performant system deduced from bibliography. Therefore, we can assume that our new developed materials are more efficient and performant for BA photodegradation than those reported in Table 2, since the surface area and the POMs quantity are minimal compared to that used in the literature.

In order to confirm BA degradation percentages calculated by UV-Visible absorption spectroscopy mass spectrometry analysis were realized at different irradiation times. The comparison between the results obtained by these two methods are shown in Figure 6 and Table 3.

Study of Bisphenol-A photodegradation in water by mass spectrometry

The kinetics of BA photodegradation by $H_3PMo_{12}O_{40}$/polymer composite was investigated by mass spectrometry. The experimental data were plotted using the logarithm of the measured concentrations ratio. the curves obtained are linear and follow the catalytic model of pseudo-first order (Figure 6) indicated by the equation (2).

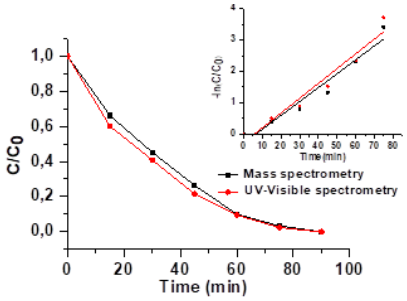

Figure 6. Study of the BA degradation kinetics under UV lamp irradiation by two different analysis methods: Mass spectrometry VS UV-visible absorption spectroscopy.

Table 3. Study of the BA degradation kinetics by two methods.

Methods	kapp (min^{-1})	R^2
UV-Visible spectrometry	0.047	0.973
Mass spectrometry	0.044	0.972

The rate constants values for photocatalytic BA degradation calculated by UV-Visible spectroscopy and mass spectrometry methods shown in Table 3, are approximatively the same which strongly confirms the exactitude of the obtained results. The final conversion percentages of BA under different irradiation sources, determined by UV-Vis spectroscopy are confirmed by mass spectrometry (Table 4, Figure 7).

Table 4. Study of the BA degradation kinetics by two methods.

Irradiation source	% of conversion of BA after irradiation	
	UV-Vis spectrometry	Mass spectrometry
UV lamp	100	100
Solar irradiation	88	89
LED@375nm	50	60

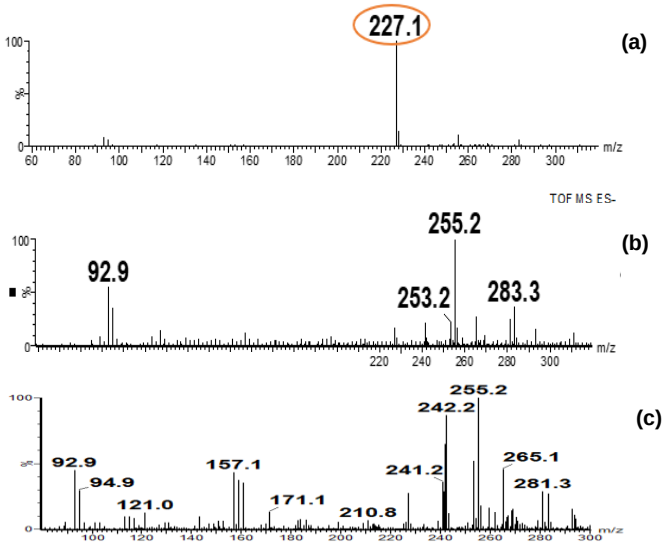

Figure 7. (a) Negative electrospray mass spectrum of the BA sample before photodegradation calibrated for exact mass measurement (targeted ion is detected at m / z=227.1) (b) High resolution mass spectrum in negative electrospray mode of the Bisphenol-A sample after photodegradation using $H_3PMo_{12}O_{40}$/polymer composite under UV lamp irradiation and (c) Negative electrospray mass spectrum of the analytical blank Study of the BA.

Table 4 and Figure 7 show that the heterogeneous photocatalytic operating under UV lamp irradiation and solar irradiation promoted the removal of BA with high efficiencies, at rates reaching 100% and 88%, respectively, after 90 min of exposure. No by-products have been identified by mass spectrometry which strongly suggest the total mineralization of this compound. In fact, the disappearance of the characteristic peak of BA at m/z=251.1 after the irradiation confirm the total degradation of this pollutant.

Mechanism of photodegradation

The samples collected during the degradation experiments were analyzed by mass spectrometry. The HRMS data and the mass spectra obtained shown in Table 5 allowed the identification of an intermediate arising from the photodegradation of BA which is the dihydroxylated Bisphenol-A (I_2). This by-product was previously reported in the literature by Xiao and coworkers who applied a nanoscale zero-valent iron/percarbonate system for BA elimination[77], by Sharma et al. who investigated BA photo-oxidation with hydrogen peroxide and sodium persulfate[78] and by few other researchers[1,79–81].

Table 5. Identification of the by-product (I_2) by mass spectrometry.

		m/z
Theoretical values		259.0976
Experimental values	1	259.0975
	2	259.0976
	3	259.0978

Based on the literature and the identified by-product, a degradation mechanism for the BA degradation could therefore be proposed as outlined in Figure 8. In fact, this photodegradation route is based on hydroxyl radical production which is in agreement with our previous works[64]. These highly reactive °OH species, react firstly with the BA aromatic ring to form I_1 and I_2. The information provided by mass spectrometry, were insufficient to establish the correct hydroxyl radical position in the chemical by-products structures. These two intermediates undergo successive hydroxylations, followed by C-C cleavage and ring opening giving linear carboxylic acids, CO_2 and H_2O.

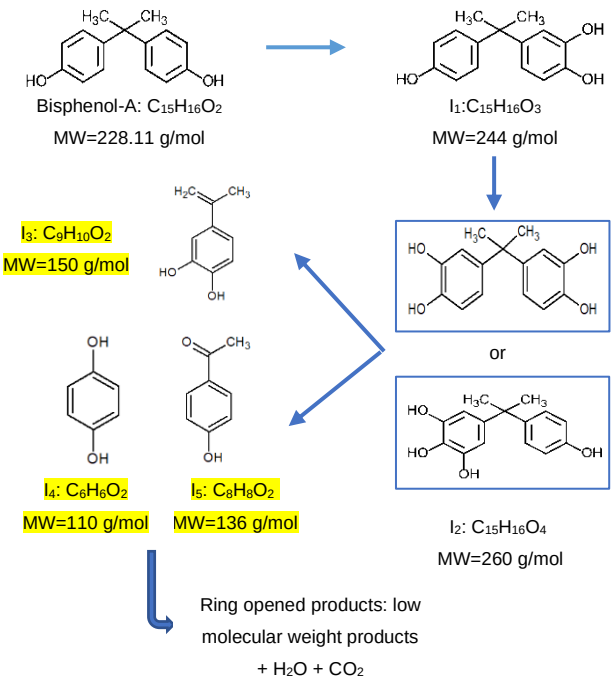

Figure 8. Proposed Bisphenol-A degradation pathways by $H_3PMo_{12}O_{40}$/polymer composite in agreement with previous studies[80–83]. The detected intermediate is I_2.

Conclusion

In our previous papers, we have reported the development under mild and simple conditions of inorganic/organic hybrid composites based on polyoxometalates by photopolymerization under visible light[64].

In this work, we investigated BA photodegradation by these new synthesized hybrid materials, under different irradiation sources and without the addition of oxidative agents in the aqueous solutions. High removal rates of this pollutant were achieved under solar and UV Lamp irradiation, thanks to the overlap of their emission spectrum with the phosphomolybdic composite absorption spectra. The total BA mineralization obtained after 90min of irradiation under UV lamp was verified by mass spectrometry analysis. Furthermore, the new developed POM/polymer composites are more efficient and performant for BA photodegradation comparing to fixed photocatalysts reported in the literature between 2000 and 2020. This conclusion was obtained by calculating ratios (D*) between the average degradation and the active surface are of the different materials. These coefficients were subsequently correlated to the initial amount of photocatalysts. Therefore, the new materials display better photocatalytic activity, since the surface area and the POMs quantity used for the POM/polymer composites synthesis are minimal compared to those used in the literature.

The degradation kinetics of this organic pollutant was also monitored by UV-Visible spectrometry and was confirmed by Mass spectrometry which furnished valuable information that allowed in addition to the literature data the identification of BA degradation mechanism pathway.

Experimental section

Chemical compounds

$H_3PMo_{12}O_{40}$[84], $W_{10}O_{32}$(Thianthrenium)$_4$[85] were synthesized according to reported procedures. The monomer trimethyl-propane triacrylate (TMPTA) used for radical polymerization was purchased from Allnex. *Bis*(4-*tert*-butylphenyl) iodonium hexafluorophosphate (Iod orSpeedcure938) and *bis*(2,4,6-trimethyl-benzoyl) phenyl-phosphine oxide (BAPO or speedcure BPO) were acquired from Lambson Ltd. Bisphenol-A (2,2-Bis(4-hydroxyphenyl) propane) was obtained from TCI and titanium dioxide was procured from

Alfa Aesar. The physiochemical properties of Bisphenol-A and titanium dioxide are reported in Table 6. The chemical structures of the reagents used in this study are given by Figure 9.

The synthesis and the characterization of the $H_3PMo_{12}O_{40}$/polymer and $W_{10}O_{32}(TH)_{44}$/polymer composites were detailed in our previous work.[64] Main properties are discussed in our previous work[65], The dimension, the BET surface area and the band gap energy of the different prepared materials are reported in Table 7.

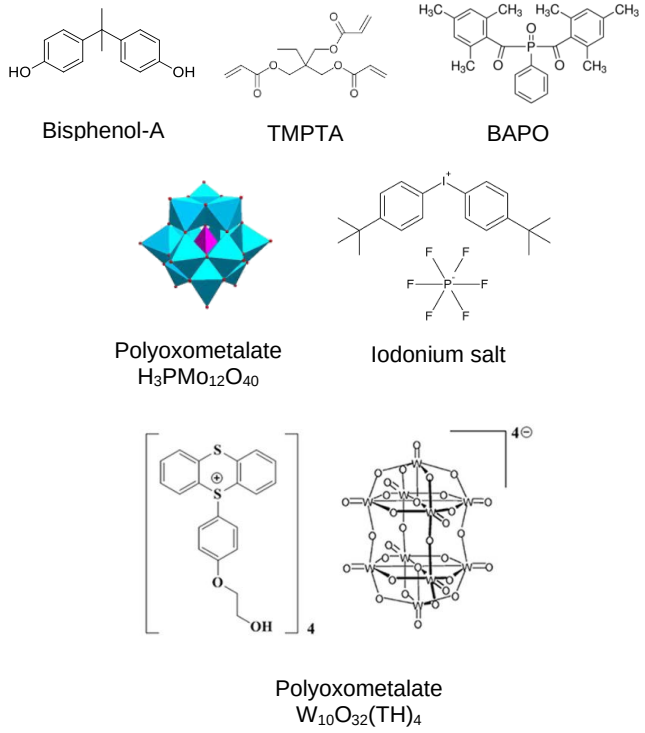

Figure 9. Chemical structures of the compounds used in this work.

Table 6. Physicochemical characteristics of Bisphenol-A and Titanium dioxide.

Compounds	Physiochemical properties	
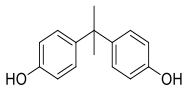	Molecular formula	$C_{15}H_{16}O_2$
	Molecular weight(g/mol)	228.287[85]
	Water solubility	120-300 mg/L at 25ºC in water[85]
	Dissociation constant (pKa)	10.29 ± 0.69[85]
	Max absorption (nm)	227-275 (η- π* transitions of the aromatic ring)[86]
	Concentration (mg. L-1)	15
	pH of the Bisphenol solution in water	6.5
	Form	White flakes or crystal[85]

Table 7. Characteristics of the developed materials[65].

Characteristics	Developed materials			
	$H_3PMo_{12}O_{40}$/ polymer	$W_{10}O_{32}(TH)_4$/ polymer	TiO_2/polymer	polymer
Band Gap Energy (e.V)	2.8	3.2	3.1	3.9
BET surface area ($m^2.g$-1)	1.3 ± 0.11	5.4 ± 0.11	-	9.3 ± 0.37

Irradiation Sources

As sources of irradiation, we have used a Light-Emitting Diodes (LED): LED@375 nm, I_0 = 70 mW/cm^2, an Omni-cure Dynamics lamp, Serie 1000 Lumen (I_0 = 250 mW/cm^2, λ=320-520 nm) and the solar irradiation (λ>290 nm). Solar photolysis has been realized on July 24, 2019 at 2 PM, in Mulhouse, France, Northeast 30°, North 47°43'46'', East 7°18'35''. The intensity of solar irradiation, measured by ''Meteo Alsace'' was equal to 766 mW/cm^2 [87]. this value corresponds to the average intesity calculated for the whole solar spectrum. However, the real intensity absorbed by photocatalysts during the photocatalytic tests was much lower than that.

Photocatalysis Experiments

Bisphenol-A samples were prepared by dissolving 15 mg in 1 L of distilled water corresponding to an initial concentration of 66µmole/L. The pH of the solution is equal to 6.5.

When experiments were carried out in the presence of POM/polymer composites, the prepared composite (pellet) were added directly in the UV-cuvette in the presence of 4 ml of the BA solution (15 ppm). In all cases, monitoring of the compound concentrations in solution over time was performed using a JASCO V730 spectrophotometer. The solutions were analyzed in a spectrophotometer cell with 1 cm path length, and data were collected in absorbance mode. The Figure 2 presents the UV-vis spectra of BA with a main absorbance at 224 nm, this absorbance will be used to monitor the conversion rate (%) related to the BA degradation in the solution.

Mass Spectroscopy Experiments

The analyzes were carried out with a SYNAPT G2 HDMS (Waters) mass spectrometer equipped with a pneumatically assisted air pressure ionization (API) source. Mass spectra (MS) were obtained with a flight time analyzer (TOF). Exact mass measurement was done in triplicate with an external calibration. The sample of treated BA solution is diluted 1/10 in a solution of methanol at 0.1mM of sodium chloride. The obtained solution is introduced into the infusion ionization source at a flow rate of 10 µl/min.

Keywords: photopolymerization, photocatalysis, sustainable chermistry, Organic-inorganic hybrid composites, Organic pollutants.

[1] J. C. C. da Silva, J. A. Reis Teodoro, R. J. de C. F. Afonso, S. F. Aquino, R. Augusti, *Rapid Commun. Mass Spectrom.* **2014**, *28*, 987–994.
[2] L. N. Vandenberg, *CMAJ* **2011**, *183*, 1265–1270.
[3] S. S. Shinde, C. H. Bhosale, K. Y. Rajpure, *Journal of Photochemistry and Photobiology B: Biology* **2014**, *141*, 186–191.
[4] R. Abo, N.-A. Kummer, B. J. Merkel, *Drinking Water Engineering and Science* **2016**, *9*, 27–35.
[5] J.-M. BRIGNON, 77, **2010**.
[6] S. Rocha, V. F. Domingues, C. Pinho, V. C. Fernandes, C. Delerue-Matos, P. Gameiro, C. Mansilha, *Bull Environ Contam Toxicol* **2013**, *90*, 73–78.
[7] B. Stachel, U. Ehrhorn, O.-P. Heemken, P. Lepom, H. Reincke, G. Sawal, N. Theobald, *Environmental Pollution* **2003**, *124*, 497–507.
[8] H.-B. Lee, T. E. Peart, *Water Quality Research Journal* **2000**, *35*, 283–298.
[9] Z. M. Nor, S. N. Yusof, H. F. Ghazi, Z. M. Isa, *Current Topics in Toxicology* **2014**, *10*, 63–70.
[10] D. Cuomo, I. Porreca, G. Cobellis, R. Tarallo, G. Nassa, G. Falco, A. Nardone, F. Rizzo, M. Mallardo, C. Ambrosino, *Molecular and Cellular Endocrinology* **2017**, *457*, 20–34.
[11] M. T. Do, V. C. Chang, M. A. Mendez, M. de Groh, *Health Promot Chronic Dis Prev Can* **2017**, *37*, 403–412.
[12] X. Gao, H.-S. Wang, *Int J Environ Res Public Health* **2014**, *11*, 8399–8413.
[13] X. Song, M. Miao, X. Zhou, D. Li, Y. Tian, H. Liang, R. Li, W. Yuan, *IJERPH* **2019**, *16*, 152.
[14] A. Ziv-Gal, J. A. Flaws, *Fertil. Steril.* **2016**, *106*, 827–856.
[15] E. Matuszczak, M. D. Komarowska, W. Debek, A. Hermanowicz, *International Journal of Endocrinology* **2019**, *2019*, 1–8.
[16] B. G. Kwon, S.-Y. Chung, K. Saido, *Environmental Research* **2020**, *191*, 110175.
[17] O. Keskinkan, B. Balci, *International Journal of Chemical Reactor Engineering* **2018**, *16*, DOI 10.1515/ijcre-2017-0125.
[18] Q. Li, F. Pan, W. Li, D. Li, H. Xu, D. Xia, A. Li, *Polymers* **2018**, *10*, 1136.
[19] C. Yang, *Water Science and Engineering* **2015**, *8*, 139–144.
[20] J. Ding, L. Bu, B. Cui, G. Zhao, Q. Gao, L. Wei, Q. Zhao, D. D. Dionysiou, *Environmental Science and Ecotechnology* **2020**, *3*, 100036.
[21] H. Gallard, A. Leclercq, J.-P. Croué, *Chemosphere* **2004**, *56*, 465–473.
[22] T. Yamamoto, A. Yasuhara, *Chemosphere* **2002**, *46*, 1215–1223.
[23] R. Mtibaà, D. R. Olicón-Hernández, C. Pozo, M. Nasri, T. Mechichi, J. González, E. Aranda, *Ecotoxicol. Environ. Saf.* **2018**, *156*, 87–96.
[24] A. Eltoukhy, Y. Jia, R. Nahurira, M. A. Abo-Kadoum, I. Khokhar, J. Wang, Y. Yan, *BMC Microbiology* **2020**, *20*, 11.
[25] E. J. Eio, M. Kawai, K. Tsuchiya, S. Yamamoto, T. Toda, *International Biodeterioration & Biodegradation* **2014**, *96*, 166–173.
[26] J. Sharma, I. M. Mishra, V. Kumar, *J. Environ. Manage.* **2015**, *156*, 266–275.
[27] J. Hu, T. Aizawa, S. Ookubo, *Environ. Sci. Technol.* **2002**, *36*, 1980–1987.
[28] T. Garoma, S. A. Matsumoto, Y. Wu, R. Klinger, *Ozone: Science & Engineering* **2010**, *32*, 338–343.
[29] P. V. L. Reddy, K.-H. Kim, B. Kavitha, V. Kumar, N. Raza, S. Kalagara, *Journal of Environmental Management* **2018**, *213*, 189–205.
[30] L. Zhao, X. Xiao, L. Peng, F. L. Gu, R. Q. Zhang, *RSC Adv.* **2014**, *4*, 10343–10349.
[31] N. P. de Moraes, R. B. Valim, R. da Silva Rocha, M. L. C. P. da Silva, T. M. B. Campos, G. P. Thim, L. A. Rodrigues, *Colloids and Surfaces A: Physicochemical and Engineering Aspects* **2020**, *584*, 124034.
[32] C.-Y. Kuo, H.-K. Jheng, S.-E. Syu, *Environmental Technology* **2019**, 1–9.
[33] P. K. Jaseela, K. O. Shamsheera, A. Joseph, *Journal of Saudi Chemical Society* **2020**, *24*, 651–662.
[34] G. Wang, J. Dai, Q. Luo, N. Deng, *Separation and Purification Technology* **2021**, *254*, 117574.
[35] G. Žerjav, M. S. Arshad, P. Djinović, J. Zavašnik, A. Pintar, *Applied Catalysis B: Environmental* **2017**, *209*, 273–284.
[36] Y. Zhu, R. Zhu, Y. Xi, T. Xu, L. Yan, J. Zhu, G. Zhu, H. He, *Chemical Engineering Journal* **2018**, *346*, 567–577.
[37] T. Ahamad, M. Naushad, Y. Alzaharani, S. M. Alshehri, *Journal of Molecular Liquids* **2020**, *311*, 113339.
[38] Y. M. Hunge, A. A. Yadav, S. Khan, K. Takagi, N. Suzuki, K. Teshima, C. Terashima, A. Fujishima, *Journal of Colloid and Interface Science* **2021**, *582*, 1058–1066.
[39] R. Guo, D. Zeng, Y. Xie, Y. Ling, D. Zhou, L. Jiang, W. Jiao, J. Zhao, S. Li, *International Journal of Hydrogen Energy* **2020**, *45*, 22534–22544.
[40] R. Liang, S. Luo, F. Jing, L. Shen, N. Qin, L. Wu, *Applied Catalysis B: Environmental* **2015**, *176–177*, 240–248.
[41] L. Jing, Y. Xu, M. Zhou, J. Deng, W. Wei, M. Xie, Y. Song, H. Xu, H. Li, *Journal of Hazardous Materials* **2020**, *396*, 122659.
[42] M. Ahmad, S. Chen, F. Ye, X. Quan, S. Afzal, H. Yu, X. Zhao, *Applied Catalysis B: Environmental* **2019**, *245*, 428–438.
[43] T. Huang, F. Tian, Z. Wen, G. Li, Y. Liang, R. Chen, *Journal of Hazardous Materials* **2021**, *403*, 123661.
[44] Y.-X. Li, X. Wang, C.-C. Wang, H. Fu, Y. Liu, P. Wang, C. Zhao, *Journal of Hazardous Materials* **2020**, *399*, 123085.
[45] K. V. A. Kumar, B. Lakshminarayana, T. Vinodkumar, Ch. Subrahmanyam, *Journal of Environmental Chemical Engineering* **2019**, *7*, 103057.
[46] M. Rani, Rachna, U. Shanker, *Environmental Technology & Innovation* **2020**, *19*, 100792.
[47] M. Rani, U. Shanker, *Journal of Colloid and Interface Science* **2018**, *530*, 16–28.
[48] J.-W. Wang, F.-G. Qiu, P. Wang, C. Ge, C.-C. Wang, *Journal of Cleaner Production* **2021**, *279*, 123408.
[49] J. M. Poblet, X. López, C. Bo, *Chem. Soc. Rev.* **2003**, *32*, 297–308.
[50] S. Valencia, J. M. Marín, G. Restrepo, *TOMSJ* **2009**, *4*, 9–14.
[51] A. Troupis, E. Gkika, A. Hiskia, E. Papaconstantinou, *Comptes Rendus Chimie* **2006**, *9*, 851–857.
[52] S. Omwoma, C. T. Gore, Y. Ji, C. Hu, Y.-F. Song, *Coordination Chemistry Reviews* **2015**, *286*, 17–29.
[53] L. Youssef, G. Younes, R. Al-Oweini, *Journal of Taibah University for Science* **2019**, *13*, 274–279.
[54] C.-G. Liu, T. Zheng, S. Liu, H.-Y. Zhang, *Journal of Molecular Structure* **2016**, *1110*, 44–52.
[55] R. Dehghani, S. Aber, F. Mahdizadeh, *Clean - Soil, Air, Water* **2018**, *46*, 1800413.
[56] A. Mylonas, E. Papaconstantinou, V. Roussis, *Polyhedron* **1996**, *15*, 3211–3217.
[57] T. R. Bastami, A. Ahmadpour, *Environ Sci Pollut Res* **2016**, *23*, 8849–8860.
[58] X.-L. Hao, Y.-Y. Ma, W.-Z. Zhou, H.-Y. Zang, Y.-H. Wang, Y.-G. Li, *Chem. Asian J.* **2014**, *9*, 3633–3640.
[59] H. Shi, T. Zhao, J. Wang, Y. Wang, Z. Chen, B. Liu, H. Ji, W. Wang, G. Zhang, Y. Li, *Journal of Alloys and Compounds* **2020**, 157924.
[60] R. Neumann, M. Levin, *J. Org. Chem.* **1991**, *56*, 5707–5710.
[61] R. R. Ozer, J. L. Ferry, *Environ. Sci. Technol.* **2001**, *35*, 3242–3246.
[62] Y. Guo, Y. Wang, C. Hu, Y. Wang, E. Wang, Y. Zhou, S. Feng, *Chem. Mater.* **2000**, *12*, 3501–3508.
[63] Y. Izumi, K. Urabe, *Chem. Lett.* **1981**, *10*, 663–666.

[64] M. Ghali, C. Brahmi, M. Benltifa, F. Dumur, S. Duval, C. Simonnet-Jégat, F. Morlet-Savary, S. Jellali, L. Bousselmi, J. Lalevée, *Journal of Polymer Science Part A: Polymer Chemistry* **2019**, *57*, 1538–1549.
[65] M. Ghali, C. Brahmi, M. Benltifa, C. Vaulot, A. Airoudj, P. Fioux, F. Dumur, C. Simonnet-Jégat, F. Morlet-Savary, S. Jellali, L. Bousselmi, J. Lalevée, *Journal of Polymer Science* **2020**, pol.20200568.
[66] H.-J. Son, C.-W. Jung, S.-H. Kim, *Environmental Engineering Research* **2008**, *13*, 197–202.
[67] G. Pirgholi-Givi, S. Farjami-Shayesteh, Y. Azizian-Kalandaragh, *Physica B: Condensed Matter* **2020**, *578*, 411886.
[68] M. A. Aguado, M. A. Anderson, C. G. Hill, *Journal of Molecular Catalysis* **1994**, *89*, 165–178.
[69] E. Papaconstantinou, M. T. Pope, *Inorg. Chem.* **1967**, *6*, 1152–1155.
[70] N. I. Gumerova, A. Rompel, *Nat Rev Chem* **2018**, *2*, 0112.
[71] H. Zhang, D. Liu, S. Ren, H. Zhang, *Res Chem Intermed* **2017**, *43*, 1529–1542.
[72] N. J. Ismail, M. H. D. Othman, S. Abu Bakar, S. H. Sheikh Abdul Kadir, M. H. Abd Aziz, M. A. B. Pauzan, S. K. Hubadillah, T. El-badawy, J. Jaafar, M. A Rahman, *Journal of Water Process Engineering* **2020**, *37*, 101504.
[73] A. Zacharakis, E. Chatzisymeon, V. Binas, Z. Frontistis, D. Venieri, D. Mantzavinos, *International Journal of Photoenergy* **2013**, *2013*, 1–9.
[74] X. Zheng, Z. Zhang, S. Meng, Y. Wang, D. Li, *Chemical Engineering Journal* **2020**, *393*, 124676.
[75] X. Kong, J. Li, C. Yang, Q. Tang, D. Wang, *Separation and Purification Technology* **2020**, *248*, 116924.
[76] C. Zhang, W. Fei, H. Wang, N. Li, D. Chen, Q. Xu, H. Li, J. He, J. Lu, *Journal of Hazardous Materials* **2020**, *399*, 123109.
[77] Y. Xiao, X. Liu, Y. Huang, W. Kang, Z. Wang, H. Zheng, *RSC Adv.* **2021**, *11*, 3636–3644.
[78] J. Sharma, I. M. Mishra, V. Kumar, *Journal of Environmental Management* **2016**, *166*, 12–22.
[79] X. Zhao, P. Du, Z. Cai, T. Wang, J. Fu, W. Liu, *Environmental Pollution* **2018**, *232*, 580–590.
[80] G. Lu, L. Zhao, M. Zhu, C. Deng, H. Liu, J. Ma, Y. Li, *Environmental Engineering Science* **2019**, *36*, 873–882.
[81] R. A. Torres-Palma, J. I. Nieto, E. Combet, C. Pétrier, C. Pulgarin, *Water Res* **2010**, *44*, 2245–2252.
[82] R. A. Torres, C. Pétrier, E. Combet, M. Carrier, C. Pulgarin, *Ultrasonics Sonochemistry* **2008**, *15*, 605–611.
[83] M. Dükkancı, *Chem. biochem. eng. q. (Online)* **2019**, *33*, 43–57.
[84] C. Rocchiccioli-Deltcheff, M. Fournier, R. Franck, R. Thouvenot, *Inorg. Chem.* **1983**, *22*, 207–216.
[85] J. Corrales, L. A. Kristofco, W. B. Steele, B. S. Yates, C. S. Breed, E. S. Williams, B. W. Brooks, *Dose-Response* **2015**, *13*, 155932581559830.
[86] L. F. Garay-Rodríguez, B. Zermeño, K. A. López de la O, E. Leyva, E. Moctezuma, L. F. Garay-Rodríguez, B. Zermeño, K. A. López de la O, E. Leyva, E. Moctezuma, *Journal of applied research and technology* **2018**, *16*, 334–345.
[87] J.-C. HERAUX-BOCQUET, “METEO ALSACE - Retrouvez nos prévisions météo en France et en Alsace à 3 jours ainsi que nos tendances à 3 mois.,” can be found under https://meteoalsace.com/, **n.d.**

Entry for the Table of Contents

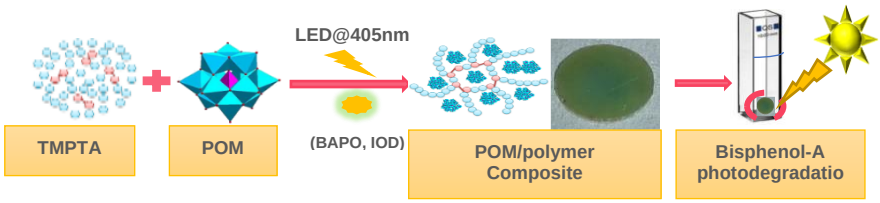

New inorganic/organic phtotocomposites based on Polyoxometalate (POM) have been successfully synthesized by photopolymerization process upon mild visible light irradiation at 405 nm. Compared to Titanium dioxide as well as the most relevant immobilized catalysts reported in the literature, these photocatalysts exhibited high catalytic activity for Bisphenol-A removal from water under solar irradiation and UV lamp irradiation.